TISSUE ENGINEERING
Volume 11, Number 7/8, 2005

Tissue Engineering of Bovine Articular Cartilage within Porous Poly(ether ester) Copolymer Scaffolds with Different Structures

TAHIR A. MAHMOOD, M.Sc.,[1–3] V. PRASAD SHASTRI, Ph.D.,[4] CLEMENS A. VAN BLITTERSWIJK, Ph.D.,[1,2] ROBERT LANGER, Sc.D.,[3] and JENS RIESLE, Ph.D.[1]

ABSTRACT

The potential of porous poly(ether ester) scaffolds made from poly(ethylene glycol) terephthalate:poly(butylene terephthalate) (PEGT:PBT) block copolymers produced by various methods to enable cartilaginous tissue formation *in vitro* was studied. Scaffolds were fabricated by two different processes: paraffin templating (PT) and compression molding (CM). To determine whether PEGT:PBT scaffolds are able to support chondrogenesis, primary bovine chondrocytes were seeded within cylindrical scaffolds under dynamic seeding conditions. On day 3, constructs were transferred to six-well plates and evaluated for glycosaminoglycan (GAG) distribution (3, 10, and 24 days), type II collagen distribution, cellularity, and total collagen and GAG content (10 and 24 days). It was observed that better cell distribution during infiltration within PT scaffolds allowed greater chondrogenesis, and at later time points, than in CM scaffolds. The amount of GAG remained constant for all groups from 10 to 24 days, whereas collagen content increased significantly. These data suggest that PEGT:PBT scaffolds are suitable for cartilage tissue engineering, with the PT process enabling greater chondrogenesis than CM.

INTRODUCTION

ARTICULAR CARTILAGE DEFECTS have been shown to have limited capacity for self-repair.[1,2] Clinically, most of these defects are found contained within the layer of cartilage, although there are also indications in which the damage penetrates deeper and into the subchondral bone. Among the techniques for repairing damaged articular cartilage is the transplantation of chondrocytes, or cartilaginous tissue that has been grown *in vitro*, to fill defect sites. This may be done by taking a tissue biopsy from the patient and isolating chondrocytes from their extracellular matrix (ECM), followed by proliferation *in vitro* before seeding onto scaffolds. Depending on the length of culture and cultivation conditions, cartilage-like tissue may be grown to varying degrees within the carrier scaffolds, which may then be implanted to fill the defect sites in cartilage.[1,3] The cartilage ECM consists predominantly of complex proteoglycan macromolecules with highly negatively charged sulfated glycosaminoglycan (GAG) side chains, as well as type II collagen fibrils. The collagenous network, together with the water-bound GAG, enables articular cartilage to withstand the large compressive loads that occur during its functional loading.[4]

A key issue in cartilage tissue engineering is the ability of the tissue-engineered construct to integrate with the

[1]IsoTis, Bilthoven, The Netherlands.
[2]Institute of Biomedical Technology, University of Twente, Enschede, The Netherlands.
[3]Division of Health Sciences and Technology, Massachusetts Institute of Technology, Cambridge, Massachusetts.
[4]Department of Biomedical Engineering, Vanderbilt University, Nashville, Tennessee.

surrounding tissue in the defect site. One approach currently being explored is to transplant constructs with less mature tissue, with the reasoning that most tissue formation should occur *in situ* and thus enable better integration with the surrounding matrix.[5] Several materials and matrices have been evaluated as carriers for chondrocyte transplantation toward the repair of articular cartilage defects (reviewed by Woodfield *et al*.[3] and Hunziker[1]). However, there are considerable issues associated with the choice of carrier matrix, among which are the ability of the matrix to withstand mechanical loads and the potentially deleterious effects of material degradation products.

Although they have been shown to be able to support chondrogenesis *in vitro*, most natural matrices such as collagen, hyaluronan, chitosan, and fibrin are unable to endure normal loading conditions.[1,3] This is also the case for several polymer hydrogels and other extensively tested porous polymer matrices such as those made of poly(glycolic acid) (PGA), poly(lactic acid) (PLA), and their copolymers (PLGA), although reports show that some PGA fiber-reinforced PLGA scaffolds exhibited considerably improved mechanical properties and success in preclinical studies.[6,7] However, these polymers biodegrade to produce acidic degradation products that may have adverse biological effects.[8,9]

Poly(ethylene glycol) terephthalate:poly(butylene terephthalate) (PEGT:PBT) copolymers have been shown to be biodegradable and biocompatible in biocompatibility studies performed both *in vitro*[10] and *in vivo*.[11,12] Overall, the copolymer properties are determined by its two components—the PEG segment is hydrophilic and provides hydrogel-like elastomeric properties, whereas PBT imparts stiffness to the system. During polymer synthesis, the molecular weight of PEG and weight ratio of the PEGT:PBT components can be defined to allow the copolymer to be tailored for desired mechanical and surface properties. We selected a composition with PEG at 300 g/mole and a PEGT:PBT ratio of 55:45, which has been previously shown to sustain chondrocyte cultures under monolayer conditions.[13] The aggregate compression modulus of porous scaffolds made of this composition has been tested to be 0.93 MPa,[14] which is close to that of normal adult articular cartilage (0.6 MPa).[15] PEGT:PBT copolymers have also been evaluated for dermal[10,11,16,17] and bone repair[18,19] applications. Furthermore, a product made from PEGT:PBT polymers has been approved for clinical use by the U.S. Food and Drug Administration.[20]

In this study, we evaluated two separate polymer-processing techniques for producing porous scaffolds from PEG:PBT. The compression-molding (CM) process utilizes the thermoplastic properties of the polymer and allows the polymer resin to melt around salt crystals inside a mold to form a porous structure.[14] On the other hand, pores are formed during the paraffin-templating (PT) process by the leaching out of paraffin porogen dissolved in a secondary solvent (hexane), during the precipitation of the polymer phase.[21] Previously, porous PLA foam-like scaffolds made by PT have been shown to support *in vitro* chondrogenesis.[21]

The objective of this study was to evaluate and compare the ability of porous PEGT:PBT scaffolds produced by different methods to form cartilaginous tissue *in vitro*.

MATERIALS AND METHODS

Scaffold preparation

PEGT:PBT polymer nomenclature: The different formulations of this copolymer system are indicated as: *a*-PEGT *b*:*c*, where *a* is the molecular weight of PEG (grams per mole), *b* is the weight percentage of PEGT, and *c* is the weight percentage of PBT. In this study, 300-PEGT 55:45 was used.

Porous scaffolds were produced using either a compression-molding (CM) or paraffin-templating (PT) technique. CM scaffolds were made by sintering PEGT:PBT polymer resin together with salt crystals at 220°C for 10 min at 20,000 lb/in^2 pressure. Scaffolds were air cooled for up to 20 min after processing and pores in the range of 400–600 μm were created by leaching out the salt crystals in H_2O.

PT scaffolds were produced as described earlier.[21] Briefly, the polymer was dissolved in methylene chloride and mixed with spherical particles (1 mm in diameter) and irregular paraffin particles of (425–500 μm in mean diameter) to yield a putty. Based on the amount of paraffin particles of each size, the theoretical average pore size was 613 μm. This putty was then packed in a Teflon mold and then extracted in hexane to yield a porous foam 1 cm^3 in volume.

Cylindrical scaffolds (4 mm in diameter and 4 mm thick) were cored out from each group, γ-sterilized under vacuum, and immersed overnight in fully supplemented medium (see components below) before cell seeding.

Cell isolation and culture

Articular cartilage was harvested from the patellar grooves of immature bovine calves. Chondrocytes were isolated by type II collagenase (Worthington Biochemical, Lakewood, NJ) digestion for 16 h and then transferred to a well-defined culture medium containing Dulbecco's modified Eagle's medium (DMEM), 10% fetal bovine serum (FBS), penicillin–streptomycin (GIBCO, Grand Island, NY), ascorbic acid phosphate, nonessential amino acids, and L-proline (Sigma, St. Louis, MO).

Once isolated, cells were seeded at a density of 3 million cells per scaffold in spinner flasks, as previously described by others.[22,23] Scaffolds were seeded under these conditions for 3 days, after which they were transferred

to six-well plates (Falcon; BD Biosciences Discovery Labware, Beford, MA) on an orbital shaker for the duration of culture. Samples from each group were harvested on day 3 for histology and on days 10 and 24 for histology, cell morphology, cellularity, collagen and GAG content, as described below.

Histology

Histological sections were obtained by fixing the polymer–tissue constructs in 2.5% glutaraldehyde and 10% formalin for 7 days. Constructs were then slowly dehydrated over 1 week in a graded ethanol series, followed by embedding in glycol methacrylate (GMA) and sectioning to a thickness of 5 μm on a standard microtome (MICROM International, Walldorf, Germany). The sections were stained with safranin O/fast green for sulfated glycosaminoglycans (GAG). Nuclei were counterstained with hematoxylin.

Scanning electron microscopy

To examine tissue-engineered construct morphology in greater detail, samples harvested on days 10 and 24 were fixed in Karnovsky's fixative, critical point dried and sputter coated with gold to a thickness of 12 nm (Cressington Scientific, Watford, UK), followed by examination by scanning electron microscopy (SEM) (ESEM; Philips, Eindhoven, The Netherlands).

Immunofluorescence microscopy

After harvesting on days 10 and 24, samples were fixed for 10 min in 10% paraformaldehyde at room temperature, infused with 15% sucrose solution, and frozen in O.C.T. compound (Tissue-Tek; Sakura Finetek Europe, Zoeterwoude, The Netherlands). Sections 7 μm thick were made on a cryotome (Thermo Shandon, Runcorn, UK) and fixed for 8 min in chilled 100% acetone. Sections were blocked for nonspecific binding by using protein block (Dako Cytomation, Glostrup, Denmark) for 1 h, followed by incubation with chicken anti-human collagen type II monoclonal antibody (Developmental Studies Hybridoma Bank, University of Iowa, Iowa City, IA) for 1 h. Sections were rinsed with phosphate-buffered saline (PBS) followed by a 30-min incubation with rabbit anti-chicken secondary antibody conjugated with Alex Fluor-488 fluorescent dye (Molecular Probes, Leiden, The Netherlands), and coverslipped with Vectashield mounting medium (Vector Laboratories, Burlingame, CA). The sections were viewed in a fluorescence microscope (Nikon, Haarlem, The Netherlands).

Quantitative GAG and collagen analyses

Constructs were harvested on days 10 and 24 and digested overnight at 56°C in a solution containing proteinase K, pepstatin A, and iodoacetamide (Sigma). Digests were evaluated for cell number, GAG, and total collagen as follows.

Cell number. Quantitation of total DNA were performed with a CyQUANT dye kit (Molecular Probes), using a spectrofluorometer (PerkinElmer, Wellesley, MA). Cell numbers were calculated from the total DNA content by normalizing to 7.7×10^{-12} g of DNA per bovine chondrocyte.[24]

GAG. GAG was quantitatively determined by labeling with dimethylmethylene blue dye (Sigma-Aldrich) and measuring color intensity with a spectrophotometer (Bio-Tek Instruments, Neufahrn, Germany).[25]

Collagen. Total collagen was determined by measuring the amount of hydroxyproline. Aliquots of proteinase K digests to be evaluated for hydroxyproline were hydrolyzed in 6 N HCl at 110°C for 16 h. The hydrolysate was assayed for hydroxyproline, using methods that have been described in detail elsewhere; a hydroxyproline content of 13% of collagen was used to calculate final collagen quantities.[26]

The data obtained from all quantitative biochemical assays were analyzed statistically by Student t test. $p < 0.05$ was used as a criterion for statistical significance. All experiments were performed in triplicate.

RESULTS

Scaffold architecture

Differences in pore structure and surface topology of scaffolds produced by PT and CM are shown in Fig. 1. The PT process resulted in a rounded and irregular pore structure (Fig. 1A), with the inner surfaces of these scaffolds exhibiting a microtextured topography (Fig. 1C). In contrast, pores in CM scaffolds were cuboidal (Fig. 1C) with smooth inner surfaces (Fig. 1D). Volumetric porosity were determined by mass–volume. Overall void volume of the CM and PT scaffolds was 78 and 80%, respectively (as determined by mass–volume calculation).

Cell distribution and matrix formation

On day 3, cell distribution was evaluated by histological observation of the construct cross-sections. Small cellular aggregates surrounded by positive safranin O staining for GAG were evident inside the pores of PT constructs (Fig. 2A). Less uniform cell infiltration was observed histologically inside CM constructs, with most safranin O staining occurred toward the outer edges of the scaffold (Fig. 2B).

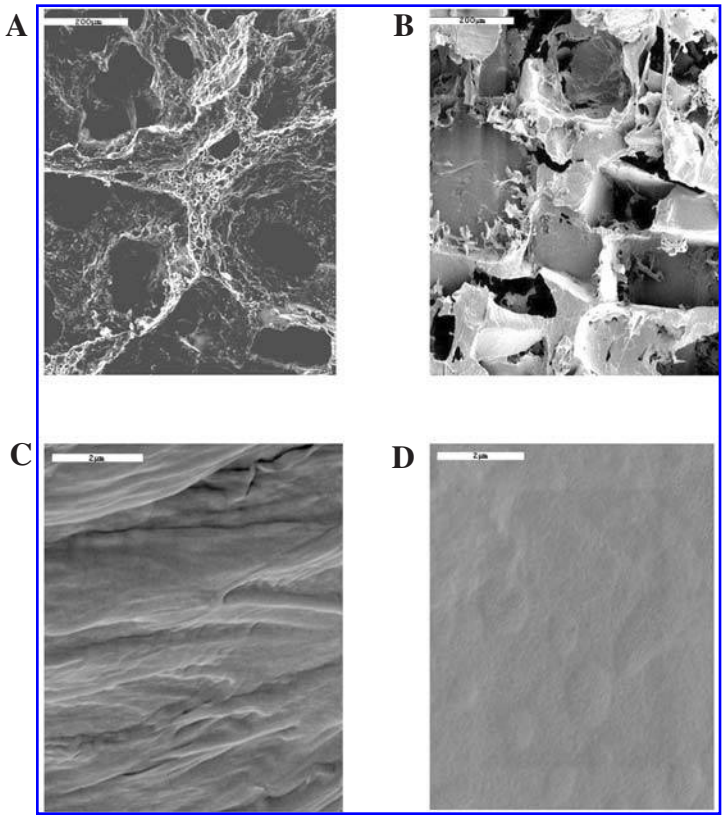

FIG. 1. Scanning electron micrographs of 300-PEG 55:45 scaffolds produced by PT (**A**) and CM (**B**) before cell seeding. PT surfaces exhibited a rougher microtopography (**C**), whereas CM surfaces were relatively smooth (**D**). Scale bars: (**A** and **B**) 200 μm; (**C** and **D**) 2 μm.

At the 10-day time point, larger regions were stained positively for safranin O in the PT constructs, as compared with day 3 (Fig. 3A) and immunofluorescence analysis revealed the presence of type II collagen (Fig. 3B). Fluorescence intensity was observed to be higher around the pericellular matrix, as compared with interstitial tissue. Polymer edges inside the constructs also exhibited some fluorescence. Scanning electron micrographs showed cells with rounded morphology embedded within a fibrillar matrix tissue within the scaffold pores (Fig. 3C).

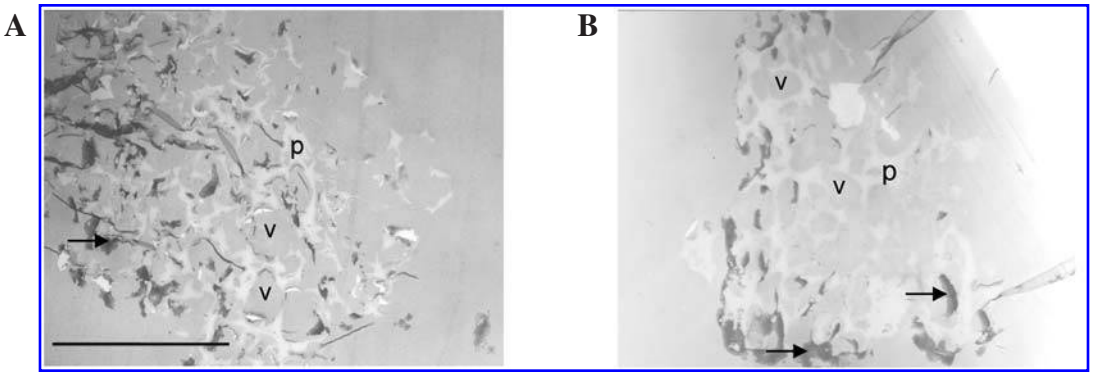

FIG. 2. Light microscopy evaluation of cross-sections of PT (**A**) and CM (**B**) constructs stained with safranin O for GAG after 3 days of dynamic seeding and culture. Scale bar: 2 mm (both images are at the same magnification). Arrows point to regions exhibiting early onset of chondrogenesis (positive safranin O staining). Polymer was not visible after histology processing, although the regions that previously contained polymer (labeled *p*) are evident because they do not contain the embedding agent GMA, and can be seen intercalating between the pores. Pore voids can be seen due to infiltration by GMA (labeled *v*).

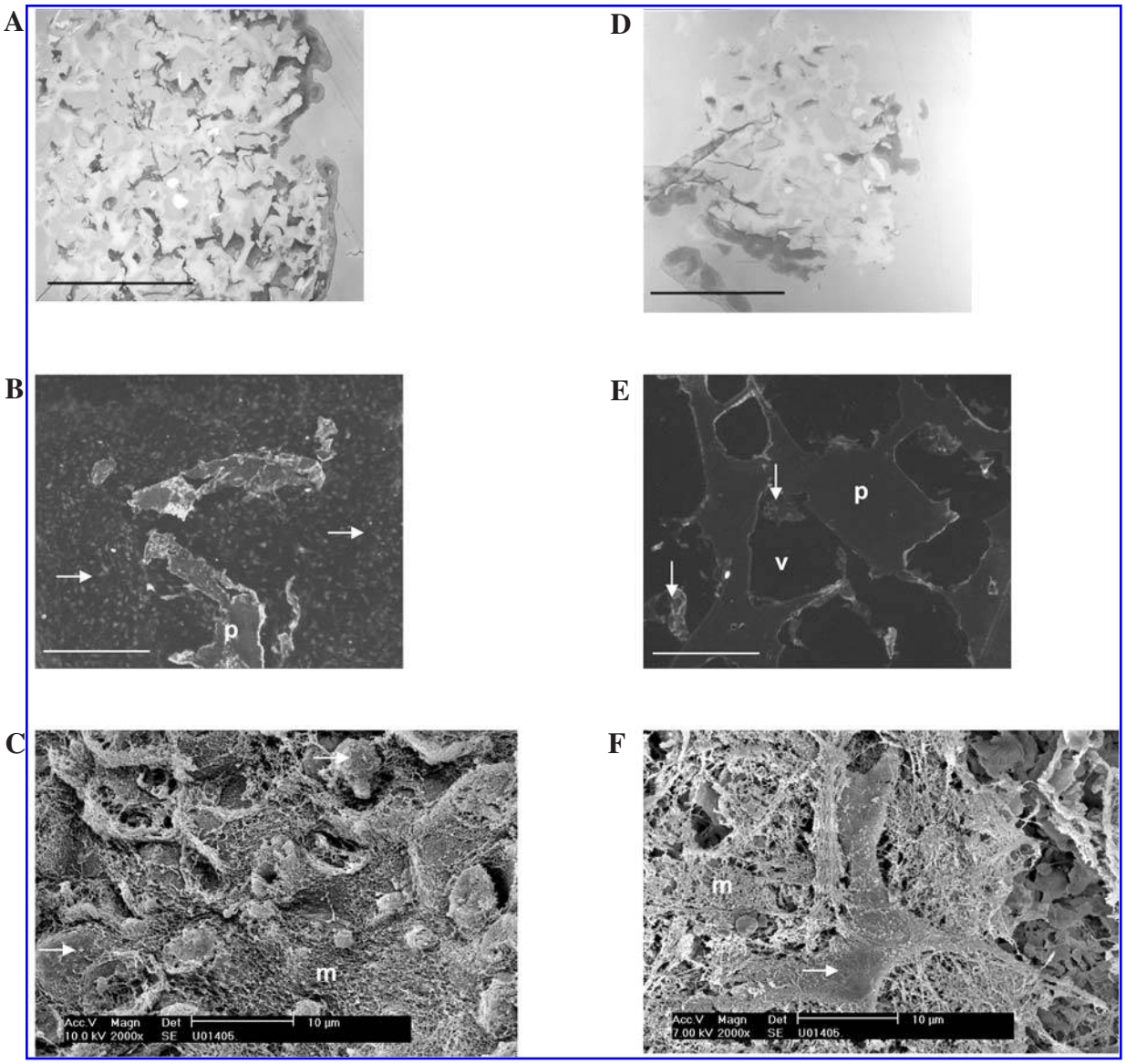

FIG. 3. Cross-sections of PT (**A–C**) and CM (**D–F**) constructs cultivated for 10 days. Sections correspond to safranin O staining (**A** and **D**), immunofluorescence labeling for type II collagen (**B** and **E**), and scanning electron micrographs (**C** and **F**). Difficulty in sectioning constructs with little tissue often necessitated taking the section toward the outer edge of the block, rather than through the construct center as in (**A**). Hence, smaller cross-sections (**D**) were obtained. Scale bars: (**A** and **D**) 2 mm; (**B** and **E**) 400 μm; (**C** and **F**) 10 μm. (**B**) *p*, fragments of polymer scaffold; arrows point to regions of positive type II collagen signal in tissue. (**E**) *p*, fragments of polymer scaffold; *v*, unfilled pore void; arrows point to regions of positive type II collagen signal in tissue. (**C**) Arrows point to rounded cells embedded in a fibrillar matrix (labeled *m*) within scaffold pores. (**F**) Arrow points to cell with a spread morphology. *m*, fibrillar matrix.

At the same time point, however, CM constructs demonstrated positive staining for GAG mainly at the scaffold periphery, and few regions of chondrogenesis in the scaffold interior (Fig. 3D). Accordingly, there was little type II collagen present and sparse matrix formation detected within the interior pores of CM scaffolds (Fig. 3E). SEM examination of tissue formation, which occurred mainly toward the scaffold periphery, often revealed cells with a spread morphology (Fig. 3F).

On day 24, safranin O staining for GAG in PT scaffolds demonstrated positively stained regions throughout the construct (Fig. 4A). Qualitatively, there was considerably higher fluorescence intensity for type II collagen in the PT constructs, as compared with the 10-day time point (Fig. 4B), and SEM examination within interior pores revealed rounded cells embedded within a fibrillar matrix (Fig. 4C).

CM scaffolds on day 24 showed limited regions within the scaffold pores staining positively for GAG

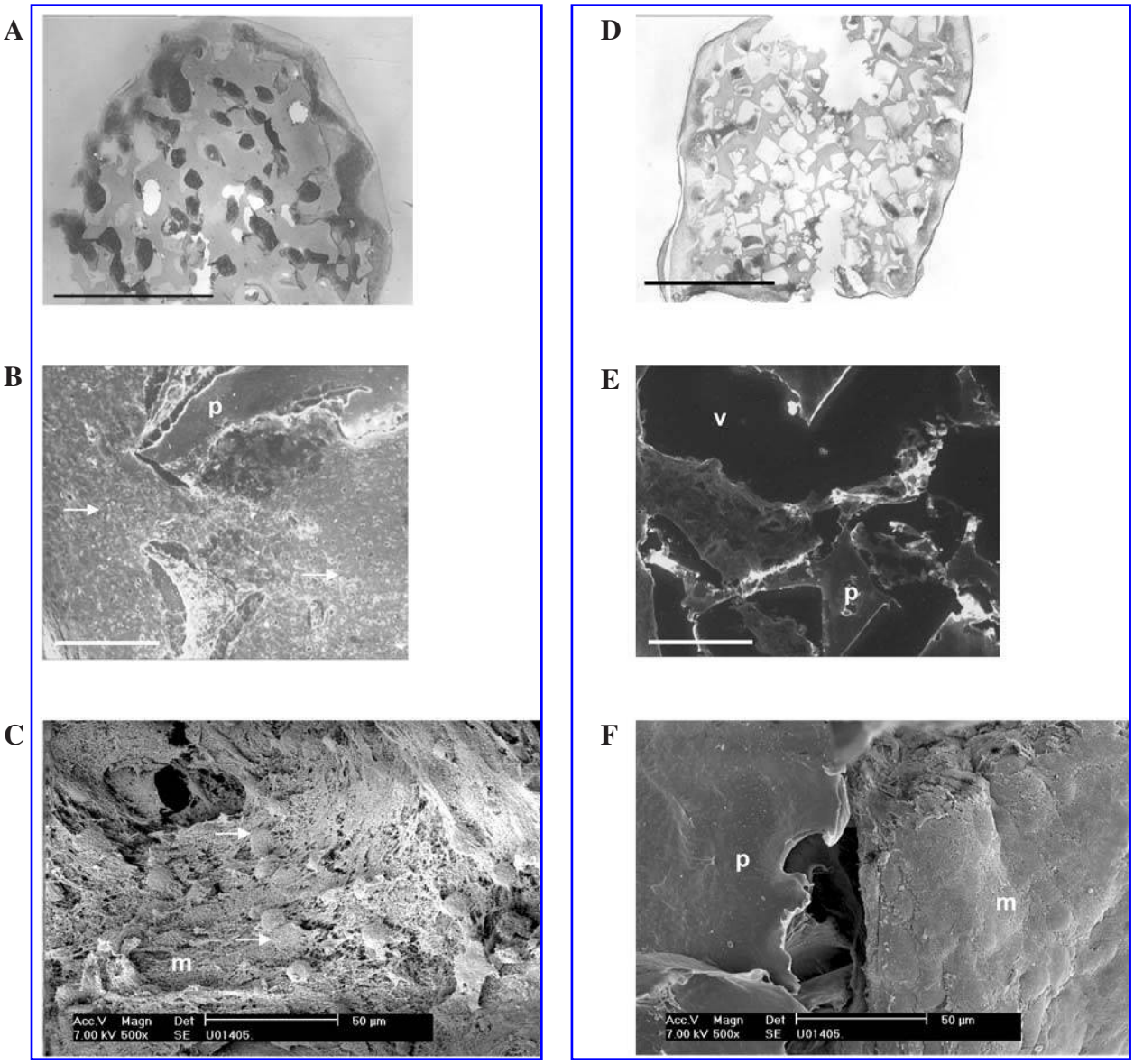

FIG. 4. Cross-sections of PT (**A**–**C**) and CM (**D**–**F**) constructs cultivated for 24 days. Sections correspond to safranin O staining (**A** and **D**), immunofluorescence labeling for type II collagen (**B** and **E**), and scanning electron micrographs (**C** and **F**). Scale bars: (**A** and **D**) 2 mm; (**B** and **E**) 400 μm; (**C** and **F**) 50 μm. (**B**) *p*, fragments of polymer scaffold; arrows point to regions of positive type II collagen signal in tissue. (**E**) *p,* fragments of polymer scaffold; *v*, unfilled pore void. (**C**) Arrows point to rounded cells embedded in a fibrillar matrix (labeled *m*) inside a scaffold pore. (**F**) *m*, tissue matrix that encapsulated scaffolds around the periphery; *p*, polymer scaffold.

with safranin O (Fig. 4D). There was little positive immunofluorescence labeling for type II collagen within the CM constructs (Fig. 4E). SEM examination showed a thick fibrous capsule around the polymer scaffold (Fig. 4F).

For some histology sections, artifacts such as folds and gaps can be seen (e.g., in Fig. 4). The folds are a consequence of sectioning polymer sections with little tissue. After repeated experiments, we have found the clear gaps to be areas where tissue used to be but was separated from the polymer scaffold and embedding material during sectioning.

Quantitative analyses

DNA assay for cell number. On day 10, PT and CM constructs contained an average of 11.6 million and 14.1 million cells per construct, respectively (Fig. 5). From 10 to 24 days, both scaffold groups displayed significant increases in cellularity (PT, $p < 0.01$; CM, $p < 0.001$). On

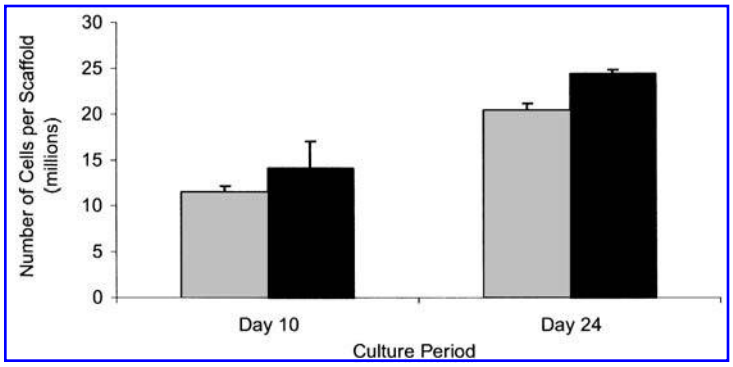

FIG. 5. Cells (millions) per construct in PT (shaded columns) and CM (solid columns) scaffolds at 10 and 24 days. Both scaffold groups exhibited a significant increase in cellularity from 10 to 24 days. The number of cells on day 24 was significantly different between scaffold types.

day 24, PT and CM constructs contained 20.4 million and 24.3 million cells, respectively. These values were significantly different ($p < 0.04$).

GAG content. At day 10, constructs were found to have an average total GAG content of $2.8 \times 10^3 \mu$g per construct (PT) and $1.9 \times 10^3 \mu$g per construct (CM), numbers that were significantly different ($p < 0.004$) (Fig. 6). Mean GAG content decreased for both scaffold types between 10 and 24 days, although this decrease was not significant for either group. On day 24, average GAG content within PT and CM constructs was 2.3×10^3 and 1.6×10^3 μg, respectively. These means were significantly different ($p < 0.003$).

Collagen content. On day 10, there was, on average, 24×10^3 μg of total collagen in PT constructs and 19.8×10^3 μg in CM constructs. There was a significant increase from day 10 to 24 for each scaffold group (PT, CM: $p < 0.0008$). On day 24, PT constructs contained significantly more collagen (66.5×10^3 μg) than did CM constructs (39.1×10^3 μg) ($p < 0.007$).

DISCUSSION

Using PT and CM techniques to process PEGT:PBT polymers resulted in scaffolds with distinct pore structures. Pores were generally rounded with PT and cuboidal with CM, because of the shapes of the porogens used in each process. However, there was inhomogeneity in pore distribution within scaffolds, as seen in the histological sections reported in this study. Comparing pore structure and void space from histologic specimens is not straightforward, however, because of technical issues inherent in the preparation of polymer–tissue constructs for histology. Void volumes for polymer scaffolds used in this study were determined by mass–volume, and are close (<3%) to values obtained by mercury porosimetry[21] and microcomputed tomography.[27]

PT scaffolds allowed a more uniform distribution of infiltrated cells than did CM scaffolds. PT scaffolds also contained greater amounts of GAG and collagen than did CM scaffolds; histology showed these compounds to be more uniformly distributed throughout the PT constructs than the CM constructs. Generally uniform cell distribu-

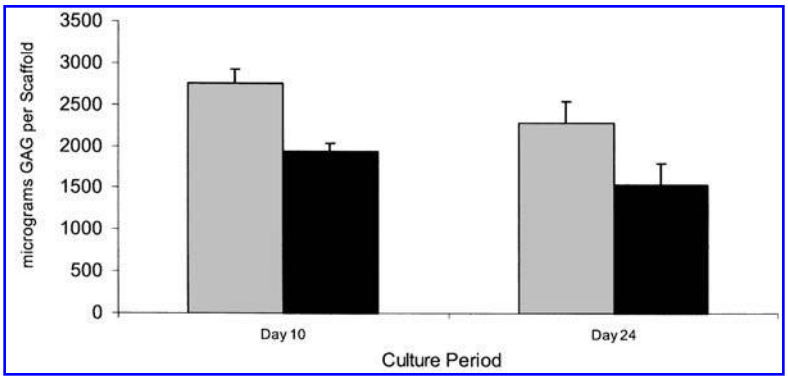

FIG. 6. GAG content (micrograms) per PT (patterned columns) and CM construct (solid columns) on days 10 and 24. GAG content in PT constructs was significantly higher than in CM groups. There was no significant change in GAG content in either scaffold type from 10 to 24 days of culture. Error bars correspond to standard deviation over the mean.

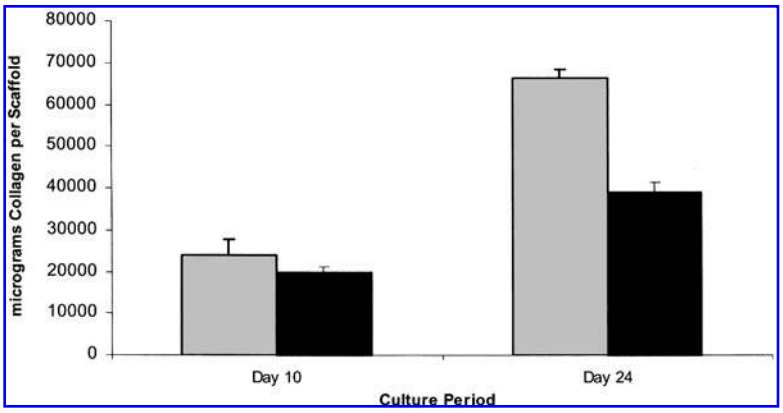

FIG. 7. Total collagen content (micrograms) per PT (patterned columns) and CM construct (solid columns) on days 10 and 24. There were significant increases in collagen content in both scaffold types from 10 to 24 days of culture. Collagen in PT constructs was also significantly higher than in CM groups on day 24. Error bars correspond to standard deviation over the mean.

tion within PT scaffolds after 3 days of seeding indicated that seeding conditions and pore geometry were suitable for cell infiltration. For CM scaffolds, however, nonuniform cell distribution suggested that CM scaffolds require further optimization in either, or both, scaffold processing and cell seeding. Even though theoretical overall volumetric porosity was similar in both scaffolds (CM, 78%; PT, 80%), different cell distribution during infiltration may partially explain the results at later time points.

In addition to the distinct pore structures, another effect of the different processing techniques was the notably different micron scale surface morphology (Fig. 1). The microtextured surfaces of PT scaffolds were likely due to efficient hexane diffusion through the polymer. It was similar to surfaces reported by others that were produced by freeze-drying in liquid nitrogen,[28] and suggests that the solvent (hexane) induced a phase-separated structure. Surface topography has been reported to influence cell function and, specifically, increased roughness reduced chondrocyte attachment, collagen production, and sulfate incorporation on two-dimensional substrates.[29,30] The fewer number of cells in the rougher-surface PT scaffolds matched this observation, because quantitative data indicated an inverse correlation between proliferation and GAG production. However, we observed increased collagen and proteoglycan production in the PT scaffolds with rougher pore surfaces than on the smooth CM scaffolds. This was likely a result of the three-dimensional scaffold environment that enhanced chondrogenic matrix production, including on rougher surfaces.

The effects of pore size on tissue formation have been described previously. Cartilaginous tissue formation was reported in scaffolds with comparatively smaller macropore diameters of 174 and 115–335 μm.[31,32] This suggests that although the mean pore sizes of both scaffolds used in the present study were large enough, it is possible that differences in pore interconnectivity or suboptimal cell seeding prevented chondrocyte infiltration within the CM scaffolds. Further analyses are required to obtain quantitative comparisons of interconnectivity and more efficient cell-seeding techniques.

The amount of GAG contained within both scaffold groups remained statistically constant during culture from day 10 to day 24. Although the average amount of GAG per scaffold decreased somewhat for each group, this was not significant. An explanation for GAG levels remaining constant may be that some of the soluble proteoglycan molecules being secreted by cells were not incorporated within the ECM, but were instead leached into the medium, as has been reported elsewhere.[33] Interestingly, the amount of GAG appeared to increase considerably between day 10 and day 24 when examined histologically. This apparent discrepancy may be explained by the location of the presented histology sections in the engineered constructs; both sections (Figs. 3A and 4A) were obtained from the center of constructs. It is possible that GAG deposited in the center of the construct was restricted in its ability to diffuse through the construct and leach out into the medium from the center, as compared with peripheral regions, because of the longer distance in all directions for the GAG to diffuse from the center and the decrease in construct permeability due to compacted tissue layers.[34] This would imply that more mobile GAG was released from the peripheral regions into the medium. This is in agreement with a phenomenon has been discussed previously, where models have demonstrated negligible GAG transport via diffusion through constructs, although GAG may be released directly into medium by cells at the periphery.[35]

The increase in quantitatively determined collagen content corresponded with immunohistochemical observation. The striking difference in collagen content on day 24 between PT and CM scaffolds is likely due to overall less cartilaginous tissue formation within CM scaf-

folds, as evidenced by GAG formation and immunohistochemistry (Fig. 4B and E). Cells that formed CM polymer–tissue constructs were unable to infiltrate scaffold interiors, and remained mainly at the periphery. As seen in Fig. 3F, many of these cells had reverted to a dedifferentiated phenotype, as evidenced by their spread morphologies. Therefore, cells that were able to infiltrate into scaffold pores and maintain their phenotype were able to form cartilaginous matrix proteins, including collagen, whereas the dedifferentiated cells may not have secreted these proteins to the same extent as the differentiated interior chondrocytes.

It has also been demonstrated that the subcutaneous implantation of PEGT:PBT scaffolds after 14 days of seeding *in vitro* resulted in markedly increased cartilaginous tissue after 4 weeks than in the *in vitro* controls,[14] suggesting that *in vivo* conditions may support more efficacious tissue repair. This study demonstrates the improved potential of PEGT:PBT scaffolds produced by PT to support *in vitro* chondrogenesis, as compared with CM. Other challenges remain, however, for the future development and potential clinical application of these technologies, including the use of human chondrocytes that have been expanded and dedifferentiated before seeding.

CONCLUSIONS

The results presented demonstrate that PEGT:PBT copolymer scaffolds can be produced by PT and CM polymer-processing techniques to produce scaffolds with similar volumetric porosity, but different pore geometries. PT scaffolds allowed better chondrocyte distribution during cell infiltration into the scaffolds, as compared with CM scaffolds, which resulted in enhanced cartilaginous tissue formation in PT scaffolds.

ACKNOWLEDGMENTS

We thank R. Haan for assistance in producing compression-molded scaffolds.

REFERENCES

1. Hunziker, E.B. Articular cartilage repair: Basic science and clinical progress. A review of the current status and prospects. Osteoarthritis Cartilage **10,** 432, 2002.
2. O'Driscoll, S.W. Preclinical cartilage repair: Current status and future perspectives. Clin. Orthop, **391,** S397, 2001.
3. Woodfield, T.B., Bezemer, J.M., Pieper, J.S., van Blitterswijk, C.A., and Riesle, J. Scaffolds for tissue engineering of cartilage. Crit. Rev. Eukaryot. Gene Expr. **12,** 209, 2002.
4. Armstrong, C.G., Lai, W.M., and Mow, V.C. An analysis of the unconfined compression of cartilage. J. Biomech. Eng. **106,** 165, 1984.
5. Obradovic, B., Martin, I., Padera, R.F., Treppo, S., Freed, L.E., and Vunjak-Novakovic, G. Integration of engineered cartilage. J. Orthop. Res. **19,** 1089, 2001.
6. Slivka, M.A., Leatherbury, N.C., Kieswetter, K., and Niederauer, G.G. Porous, resorbable, fiber-reinforced scaffolds tailored for articular cartilage repair. Tissue Eng. **7,** 767, 2001.
7. Niederauer, G.G., Slivka, M.A., Leatherbury, N.C., Korvick, D.L., Harroff, H.H., Ehler, W.C., Dunn, C.J., and Kieswetter, K. Evaluation of multiphase implants for repair of focal osteochondral defects in goats. Biomaterials **21,** 2561, 2000.
8. Spain, T.L., Agrawal, C.M., and Athanasiou, K.A. New technique to extend the useful life of a biodegradable cartilage implant. Tissue Eng. **4,** 343, 1998.
9. Athanasiou, K.A., Agrawal, C.M., Barber, F.A., and Burkhart, S.S. Orthopaedic applications for PLA–PGA biodegradable polymers. Arthroscopy **14,** 726, 1998.
10. van Dorp, A.G., Verhoeven, M.C., Koerten, H.K., van Blitterswijk, C.A., and Ponec, M. Bilayered biodegradable poly(ethylene glycol)/poly(butylene terephthalate) copolymer (Polyactive) as substrate for human fibroblasts and keratinocytes. J. Biomed. Mater. Res. **47,** 292, 1999.
11. Beumer, G.J., van Blitterswijk, C.A., and Ponec, M. Biocompatibility of a biodegradable matrix used as a skin substitute: An *in vivo* evaluation. J. Biomed. Mater. Res. **28,** 545, 1994.
12. Beumer, G.J., van Blitterswijk, C.A., and Ponec, M. Degradative behaviour of polymeric matrices in (sub)dermal and muscle tissue of the rat: A quantitative study. Biomaterials **15,** 551, 1994.
13. Papadaki, M., Mahmood, T., Gupta, P., Claase, M.B., Grijpma, D.W., Riesle, J., van Blitterswijk, C.A., and Langer, R. The different behaviors of skeletal muscle cells and chondrocytes on PEGT/PBT block copolymers are related to the surface properties of the substrate. J. Biomed. Mater. Res. **54,** 47, 2001.
14. Malda, J., Woodfield, T.B., van der Vloodt, F., Wilson, C., Martens, D.E., Tramper, J., van Blitterswijk, C.A., and Riesle, J. The effect of PEGT/PBT scaffold architecture on the composition of tissue engineered cartilage. Biomaterials **26,** 63, 2005.
15. Treppo, S., Koepp, H., Quan, E.C., Cole, A.A., Kuettner, K.E., and Grodzinsky, A.J. Comparison of biomechanical and biochemical properties of cartilage from human knee and ankle pairs. J. Orthop. Res. **18,** 739, 2000.
16. Beumer, G.J., van Blitterswijk, C.A., Bakker, D., and Ponec, M. A new biodegradable matrix as part of a cell seeded skin substitute for the treatment of deep skin defects: A physico-chemical characterisation. Clin. Mater. **14,** 21, 1993.
17. Van Dorp, A.G., Verhoeven, M.C., Koerten, H.K., Van Der Nat-Van Der Meij, T.H., Van Blitterswijk, C.A., and Ponec, M. Dermal regeneration in full-thickness wounds in Yucatan miniature pigs using a biodegradable copolymer. Wound Repair Regen. **6,** 556, 1998.
18. Radder, A.M., Leenders, H., and van Blitterswijk, C.A. Application of porous PEO/PBT copolymers for bone replacement. J. Biomed. Mater. Res. **30,** 341, 1996.
19. Sakkers, R.J., Dalmeyer, R.A., de Wijn, J.R., and van Blit-

terswijk, C.A. Use of bone-bonding hydrogel copolymers in bone: An *in vitro* and *in vivo* study of expanding PEO–PBT copolymers in goat femora. J. Biomed. Mater. Res. **49,** 312, 2000.
20. U.S. Food and Drug Administration. Approval Notice Number K010840, 2001.
21. Shastri, V.P., Martin, I., and Langer, R. Macroporous polymer foams by hydrocarbon templating. Proc. Natl. Acad. Sci. U.S.A. **97,** 1970, 2000.
22. Freed, L.E., Hollander, A.P., Martin, I., Barry, J.R., Langer, R., and Vunjak-Novakovic, G. Chondrogenesis in a cell–polymer–bioreactor system. Exp. Cell Res. **240,** 58, 1998.
23. Freed, L.E., Vunjak-Novakovic, G., and Langer, R. Cultivation of cell–polymer cartilage implants in bioreactors. J. Cell Biochem. **51,** 257, 1993.
24. Kim, Y.J., Sah, R.L., Doong, J.Y., and Grodzinsky, A.J. Fluorometric assay of DNA in cartilage explants using Hoechst 33258. Anal. Biochem. **174,** 168, 1988.
25. Farndale, R.W., Buttle, D.J., and Barrett, A.J. Improved quantitation and discrimination of sulphated glycosaminoglycans by use of dimethylmethylene blue. Biochim. Biophys. Acta **883,** 173, 1986.
26. Morales, T.I., Woessner, J.F., Howell, D.S., Marsh, J.M., and LeMaire, W.J. A microassay for the direct demonstration of collagenolytic activity in Graafian follicles of the rat. Biochim. Biophys. Acta. **524,** 428, 1978.
27. Miot, S., Woodfield, T., Daniels, A.U., Suetterlin, R., Peterschmitt, I., Heberer, M., van Blitterswijk, C. A., Riesle, J., and Martin, I. Effects of scaffold composition and architecture on human nasal chondrocyte redifferentiation and cartilaginous matrix deposition. Biomaterials **26,** 2479, 2005.
28. Schugens, C.H., Maquet, V., Grandfils, C., Jerome, R., and Teyssie, P.H. Biodegradable and macroporous polylactide implants for cell transplantation. 1. Preparation of macroporous polylactide supports by solid-liquid phase separation. Polymer **37,** 1027, 1996.
29. Hambleton, J., Schwartz, Z., Khare, A., Windeler, S.W., Luna, M., Brooks, B.P., Dean, D.D., and Boyan, B.D. Culture surfaces coated with various implant materials affect chondrocyte growth and metabolism. J. Orthop. Res. **12,** 542, 1994.
30. Boyan, B.D., Hummert, T.W., Dean, D.D., and Schwartz, Z. Role of material surfaces in regulating bone and cartilage cell response. Biomaterials **17,** 137, 1996.
31. Miralles, G., Baudoin, R., Dumas, D., Baptiste, D., Hubert, P., Stoltz, J.F., Dellacherie, E., Mainard, D., Netter, P., and Payan, E. Sodium alginate sponges with or without hyaluronate: *In vitro* engineering of cartilage. J. Biomed. Mater. Res. **57,** 268, 2001.
32. LiVecchi, A.B., Tombes, R.M., and LaBerge, M. *In vitro* chondrocyte collagen deposition within porous HDPE: Substrate microstructure and wettability effects. J. Biomed. Mater. Res. **28,** 839, 1994.
33. van Susante, J.L.C., Pieper, J., Buma, P., van Kuppevelt, T.H., van Beuningen, H., van Der Kraan, P.M., Veerkamp, J.H., van den Berg, W. B., and Veth, R.P.H. Linkage of chondroitin-sulfate to type I collagen scaffolds stimulates the bioactivity of seeded chondrocytes *in vitro*. Biomaterials **22,** 2359, 2001.
34. Freed, L.E., Vunjaknovakovic, G., Marquis, J.C., and Langer, R. Kinetics of chondrocyte growth in cell–polymer implants. Biotechnol. Bioeng. **43,** 597, 1994.
35. Obradovic, B., Meldon, J.H., Freed, L.E., and Vunjak-Novakovic, G. Glycosaminoglycan deposition in engineered cartilage: Experiments and mathematical model. AIChE J. **46,** 1860, 2000.

Address reprint requests to:
Clemens van Blitterswijk, Ph.D.
University of Twente, IsoTis SA
Bilthoven Research Group
Prof. Bronkhorstlaan 10
Bilthoven 3723 MB, The Netherlands

E-mail: C.A.vanBlitterswijk@tnw.utwente.nl

This article has been cited by:

1. J Sohier, L Moroni, C van Blitterswijk, K de Groot, JM Bezemer. 2008. Critical factors in the design of growth factor releasing scaffolds for cartilage tissue engineering. *Expert Opinion on Drug Delivery* **5**:5, 543-566. [CrossRef]
2. Jojanneke M. Jukes, Lorenzo Moroni, Clemens A. van Blitterswijk, Jan de Boer. 2008. Critical Steps toward a Tissue-Engineered Cartilage Implant Using Embryonic Stem Cells. *Tissue Engineering* **14**:1, 135-147. [CrossRef]
3. Jojanneke M. Jukes , Lorenzo Moroni , Clemens A. van Blitterswijk , Jan de Boer . 2008. Critical Steps toward a Tissue-Engineered Cartilage Implant Using Embryonic Stem CellsCritical Steps toward a Tissue-Engineered Cartilage Implant Using Embryonic Stem Cells. *Tissue Engineering Part A* **14**:1, 135-147. [Abstract] [PDF] [PDF Plus]
4. Lorenzo Moroni , Maurus Curti , Manfred Welti , Stephen Korom , Walter Weder , Joost R. de Wijn , Clemens A. van Blitterswijk . 2007. Anatomical 3D Fiber-Deposited Scaffolds for Tissue Engineering: Designing a NeotracheaAnatomical 3D Fiber-Deposited Scaffolds for Tissue Engineering: Designing a Neotrachea. *Tissue Engineering* **13**:10, 2483-2493. [Abstract] [PDF] [PDF Plus]
5. Tahir A. Mahmood, V. Prasad Shastri, Clemens A. van Blitterswijk, Robert Langer, Jens Riesle. 2006. Evaluation of chondrogenesis within PEGT: PBT scaffolds with high PEG content. *Journal of Biomedical Materials Research Part A* **79A**:1, 216-222. [CrossRef]